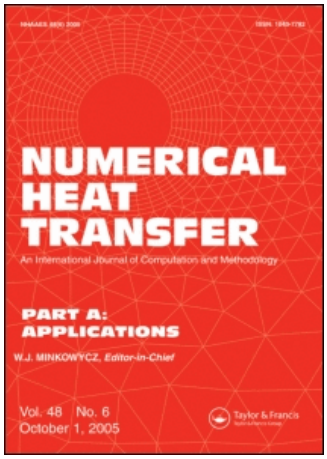

Numerical Heat Transfer, Part A: Applications
An International Journal of Computation and Methodology
Publication details, including instructions for authors and subscription information:
http://www.informaworld.com/smpp/title~content=t713657973

The Influence of Strip Location on the Pressure Drop and Heat Transfer Performance of a Slotted Fin

W. Q. Tao [a]; Y. P. Cheng [b]; T. S. Lee [b]
[a] School of Energy and Power Engineering, Xi'an Jiaotong University, Xi'an, People's Republic of China
[b] Laboratory of Fluid Mechanics, Department of Mechanical Engineering, National University of Singapore, Singapore

Online Publication Date: 01 January 2007
To cite this Article: Tao, W. Q., Cheng, Y. P. and Lee, T. S. (2007) 'The Influence of Strip Location on the Pressure Drop and Heat Transfer Performance of a Slotted Fin', Numerical Heat Transfer, Part A: Applications, 52:5, 463 - 480
To link to this article: DOI: 10.1080/10407780701301652
URL: http://dx.doi.org/10.1080/10407780701301652

Numerical Heat Transfer, Part A, 52: 463–480, 2007

ISSN: 1040-7782 print/1521-0634 online
DOI: 10.1080/10407780701301652

THE INFLUENCE OF STRIP LOCATION ON THE PRESSURE DROP AND HEAT TRANSFER PERFORMANCE OF A SLOTTED FIN

W. Q. Tao
School of Energy and Power Engineering, Xi'an Jiaotong University, Xi'an, People's Republic of China

Y. P. Cheng and T. S. Lee
Laboratory of Fluid Mechanics, Department of Mechanical Engineering, National University of Singapore, Singapore

In this article, a numerical study is conducted to predict the air-side heat transfer and pressure drop characteristics of slit fin-and-tube heat transfer surfaces. A three-dimensional steady laminar model is applied, and the heat conduction in the fins is also considered. Five types of slit fins, named slit 1, slit 2, slit 3, slit 4, and slit 5, are investigated, which have the same global geometry dimensions and the same numbers of strips on the fin surfaces. The only difference among the five slit fins lies in the strip arrangement. Slit 1 has all the strips located in the front part of the fin surface, then, following the order from slit 1 to slit 5, the strip number in the front part decreases and, correspondingly, the strip number in the rear part increases, so that all the strips of slit 5 are located in the rear part. Furthermore, slit 1 and slit 5, slit 2 and slit 4, have a symmetrical strip arrangement along the flow direction. The numerical results show that, following the order from slit 1 and slit 5, the heat transfer rate increases at first, reaching a maximum value at slit 3, which has the strip arrangement of "front coarse and rear dense"; after that, it begins to decrease, as does the fin efficiency. Although they have the symmetrical strip arrangement along the flow direction, slit 5 has 7% more Nusselt number than slit 1, and slit 4 also has 7% more Nusselt number than slit 2, which shows that strip arrangement in the rear part is more effective than that in the front part. Then the difference of heat transfer performance among five slit fins is analyzed from the viewpoint of thermal resistance, which shows that when the thermal resistances in the front and rear parts are nearly identical, the optimum enhanced heat transfer fin can be obtained. This quantitative rule, in conjunction with the previously published qualitative principle of "front sparse and rear dense," can give both quantitative and qualitative guides to the design of efficient slotted fin surfaces. Finally, the influence of fin material on the performance of enhanced-heat-transfer fins is discussed.

Received 15 May 2006; accepted 29 January 2007.
This work was supported by the National Key Project of Fundamental R&D of China (Grant 2007CB206902) and the National Natural Science Foundation of China (Grant 50476046).
Address correspondence to Wen-Quan Tao, State Key Laboratory of Multiphase Flow in Power Engineering, School of Energy and Power Engineering, Xi'an Jiaotong University, Xi'an, Shaanxi 710049, People's Republic of China. E-mail: wqtao@mail.xjtu.edu.cn

NOMENCLATURE

A	heat transfer area, m^2	v	velocity in y direction, m/s
c_p	specific heat at constant pressure, kJ/kg K	w	velocity in z direction, m/s
		Γ	diffusion coefficient ($= \lambda/c_p$)
D_e	outer tube diameter, m	η	fin efficiency
f	friction factor	λ	thermal conductivity, W/m K
h	heat transfer coefficient, W/m^2 K	μ	dynamic viscosity, kg/m s
L	fin depth in air flow direction, m	ρ	air density, kg/m^3
Δp	pressure drop, Pa		
Q	heat transfer rate, W	**Subscripts**	
R	thermal resistance, K/W	in	inlet
Re	Reynolds number	m	mean
T	temperature, K	max	maximum
ΔT	log-mean temperature difference, K	min	minimum
		out	outlet
u	velocity in x direction, m/s	w	wall

INTRODUCTION

Plate fin-and-tube heat exchangers, as shown in Figure 1, are widely used in various engineering fields, such as heating, ventilation, air conditioning, and refrigeration (HVAC&R) and air intercoolers. The cooling water or refrigerant usually flows in the tubes, and the air passes through the passages between the two adjacent fins. As the air-side thermal resistance often accounts for about 90% of the overall thermal resistance, it is necessary to reduce it by adopting enhanced-heat-transfer fins. Generally, there are three types of plate-fin surface: plain plate fins, corrugated plate fins, and slotted fins. Because of the excellent performance of the slotted fin, it has gained considerable attention and seen increasing use. According to recent investigations [1–4], the essence of heat transfer enhancement of the slotted fin is attributed to the improvement of the synergy between the velocity and the temperature field.

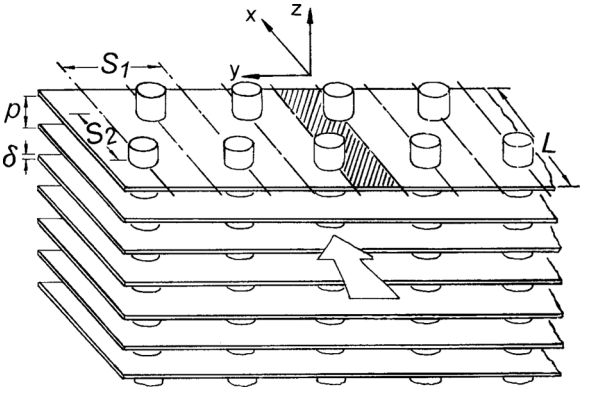

Figure 1. Schematic diagram of a fin-and-tube heat exchanger.

The slotted fin class includes the louvered fin and the slit fin with protruding strips. The louvered fin surface has very high heat transfer coefficient, but its pressure drop penalty is sometimes so great that prevents its wide application. For example, Yun and Lee [5] used a scaled-up model in their experiment and compared the performance of the plain fin, louvered fin, and three slit fins, and the results showed that all the slit fins have greater j factor and smaller f factor than those of the louvered fin. The better performance of the slit fin than the louvered fins is also demonstrated in the study by Kang et al. [6]

The slit fin was first studied by Nakayama and Xu [7], who presented test results for three samples, based on which a correlation on heat transfer and friction factor was developed. They also reported that the heat transfer coefficient can be 78% higher than that of the plain fin at 3-m/s air velocity. Later, Hiroaki et al. [8] also investigated experimentally three kinds of slit fins with a high density of strips and an X-shape arrangement. Their results indicated that the heat exchanger with the slit fin can have one-third less volume than that with the plain fin. Recently, Wang et al. [9] and Du and Wang [10] did a systematic experimental investigation of the slit fin with tens of samples, and provided experimental correlations of heat transfer and friction factor. Besides the investigation of the performance of the whole fin surface, there is also some research on particular geometry parameters. Yun and Lee [11] analyzed the effects of various design parameters on the heat transfer and pressure drop characteristics of the heat exchanger with slit fins, and they also presented the optimum value of each parameter. Kang and Kim [12] studied the effect of strip location on the heat transfer and pressure drop; according to their experimental results, the slit fin with all the strips located in the rear part of the fin surface has higher heat transfer rate and lower pressure drop than that with all the strips located in the front part.

Because of the complex geometry configuration, it is very expensive and time-consuming to perform a comprehensive investigation of the performance of a slit fin surface by experiment. For example, in order to develop the correlations of heat transfer and friction characteristics, Du and Wang [10] considered 50 slit fins with different geometry dimensions. However, with the emergence of computers with high speed and large memory, numerical modeling, once validated by some test data, becomes a cost-effective and time-saving method to carry out such a parametric study.

Sheui et al. [13] conducted a numerical investigation of the slotted fin with parallel strips and wavy strips in early time. By virtue of topological study, they did a thorough study on the flow. Recently, Qu et al. [3] simulated four types of fins with the same geometry dimensions as those used in Kang and Kim's experiments, and their results agreed well with the experimental results. Furthermore, Qu et al. also explained why the slit fin with all the strips on the rear part gives better performance than that with all the strips on the front part, from the viewpoint of the field synergy principle [1, 2]. They reported that the better performance lies in the better synergy between the velocity and the temperature gradient. According to this principle, Cheng et al. [4] designed an efficient slit fin with the strip arrangement of "front sparse and rear dense." However, for the engineering application of this principle, it is required to give some quantitative description of the strip location arrangement. In this article, the influence of strip arrangement on the heat transfer and friction performance is analyzed in detail, and apart from the principle of "front sparse

and rear dense," the heat transfer rate of a slotted fin surface is analyzed from the viewpoint of thermal resistance. With the method introduced in this article, an efficient slit fin can be designed more easily, instead through a purely empirical trial-and-error method. The effect of thermal conductivity on the heat transfer enhancement is also given and explained.

In the following presentation, the physical model and numerical formulation for five different types of slit fins is first presented, followed by detailed descriptions of the numerical treatment. Then, numerical results are provided. In this part, focus is first put on the reliability of the physical model and the code is developed, then a comparison among five types of slit fins is conducted and their heat transfer performance is analyzed from the viewpoint of thermal resistance. The influence of fin material on the heat transfer performance is also addressed. Finally, some conclusions are drawn which will be helpful in the design of new enhancement surfaces.

PHYSICAL MODEL

The geometry of five types of slit fins used in air intercoolers is shown in Figure 2. There are three tube rows along the flow direction, which are arranged in a staggered way. For all five slit fins, the global geometries are of the same dimension. Along the flow direction there are 10 lines of strips, which protrude upwind and downward alternatively, and in the same numbering line the total spanwise length of the strips is also approximately the same. The only difference among the five slit fins lies in the strip arrangement on the fin surface. Slit 1 has all the strips located in the front part of the fin surface. Following the order from slit 1 to slit 5, the strip number in the front part decreases and, correspondingly, the strip number in the rear part increases, so that all the strips of slit 5 are located in the rear part. Furthermore, slit 1 and slit 5, slit 2 and slit 4 have symmetrical strip arrangements along the flow direction. The cooling water goes through inside the tubes, and the air to be cooled flows along the fin surfaces. The heat is transmitted from the air to the tube wall and the fin surface, then to the cooling water. Because the heat transfer coefficient between the cooling water and the inner wall of the tube is quite high, and the tube and the fin are made of copper, which has high thermal conductivity, the tube is assumed to be at constant temperature. However, the temperature distribution in the fin surface is to be calculated, so the problem is conjugated in that both the temperature in the fin surface and in the fluid are to be determined simultaneously [14]. In the numerical simulation, the air is assumed to be incompressible and dry with constant physical properties, and a three-dimensional steady laminar model is adopted. The numerical simulation is carried out under dry condition, hence there is no any water vapor condensation at the tube surface. The detailed geometries of the five slit fins simulated are presented in Table 1.

MATHEMATICAL FORMULATION

Computational Domain

Figure 3 shows the computational domain for slit 3. Here x is set as the streamwise coordinate, y as the spanwise coordinate, and z as the fin pitch direction.

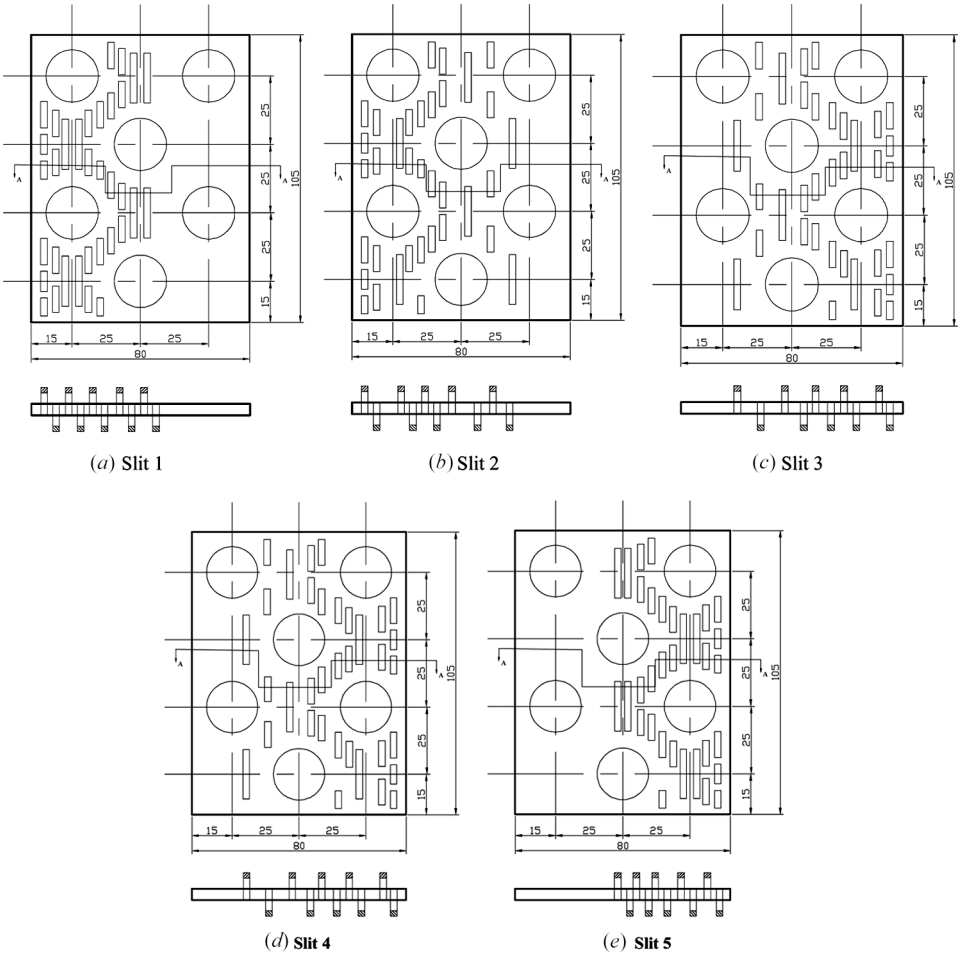

Figure 2. Geometry configuration of five patterns of slit arrangement.

Because of the geometry characteristics of symmetry and period, the computational domain is the region between the centerline of two adjacent tubes in the y direction and between the middle of two neighboring fins in the z direction. It should be noted

Table 1. Simulation conditions

Tube outside diameter	19.1 mm
Longitudinal tube pitch	25.0 mm
Transverse tube pitch	25.0 mm
Fin thickness	0.3 mm
Fin pitch	2.5 mm
Strip width	2.0 mm
Strip height	1.25 mm
Tube temperature	308 K
Inlet air temperature	403 K
Inlet frontal velocity	2–10.0 m/s

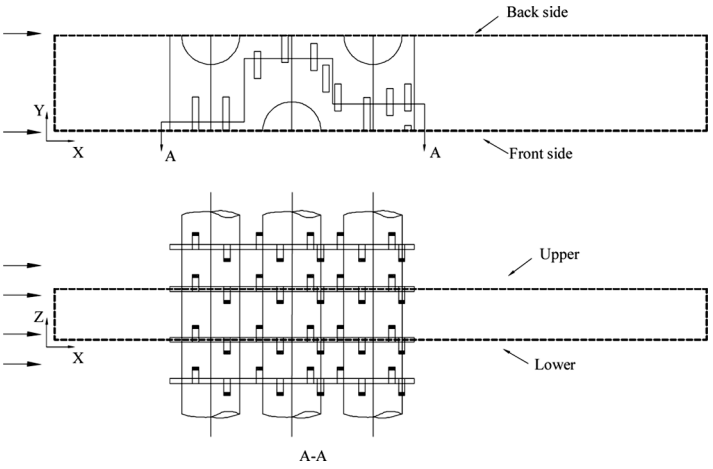

Figure 3. Computational domain of slit 3.

that in the x direction the computational domain is extended upstream 1.5 times the streamwise fin length so that a uniform velocity distribution can be assigned at the inlet. At the same time, the domain is extended downstream 10 times the streamwise fin length, so the recirculation will not appear in the domain outlet, and the one-way coordinate assumption can be adopted there.

Governing Equations and Boundary Conditions

The governing equations for continuity, momentum, and energy in the computational domain can be expressed as follows.

Continuity equation:

$$\frac{\partial}{\partial x_i}(\rho u_i) = 0 \tag{1}$$

Momentum equations:

$$\frac{\partial}{\partial x_i}(\rho u_i u_k) = \frac{\partial}{\partial x_i}\left(\mu \frac{\partial u_k}{\partial x_i}\right) - \frac{\partial p}{\partial x_k} \tag{2}$$

Energy equation:

$$\frac{\partial}{\partial x_i}(\rho u_i T) = \frac{\partial}{\partial x_i}\left(\Gamma \frac{\partial T}{\partial x_i}\right) \tag{3}$$

where $\Gamma = \lambda / c_p$.

Because the governing equations are elliptic, boundary conditions are required for all boundaries of the computational domain. The required conditions are described for the three regions as follows.

1. In the upstream extended region (domain inlet)

At the inlet: $u = \text{const} \quad T_{\text{in}} = \text{const} \quad v = w = 0$ (4*a*)

At the upper and lower boundaries: $\dfrac{\partial u}{\partial z} = \dfrac{\partial v}{\partial z} = 0 \quad w = 0 \quad \dfrac{\partial T}{\partial z} = 0$ (4*b*)

At the front and back sides: $\dfrac{\partial u}{\partial y} = \dfrac{\partial w}{\partial y} = 0 \quad v = 0 \quad \dfrac{\partial T}{\partial y} = 0$ (4*c*)

2. In the downstream extended region (domain outlet)

At the upper and lower boundaries: $\dfrac{\partial u}{\partial z} = \dfrac{\partial v}{\partial z} = 0 \quad w = 0 \quad \dfrac{\partial T}{\partial z} = 0$ (5*a*)

At the front and back sides: $\dfrac{\partial u}{\partial y} = \dfrac{\partial w}{\partial y} = 0 \quad v = 0 \quad \dfrac{\partial T}{\partial y} = 0$ (5*b*)

At the outlet boundary: one-way coordinate assumption

3. In the fin coil region
At the upper and lower surfaces:

Velocity at solid: $u = v = w = 0$ (6*a*)

Velocity of the fluid in the slits: periodic conditions

Temperature for both solid and fluid: periodic conditions

At the front and back sides:

Fluid region: $\dfrac{\partial u}{\partial y} = \dfrac{\partial w}{\partial y} = 0 \quad v = 0 \quad \dfrac{\partial T}{\partial y} = 0$ (6*b*)

Fin surface region: $u = v = w = 0$ (6*c*)

Tube region: $u = v = w = 0 \quad T_w = \text{const}$ (6*d*)

Temperature condition for both fin and fluid regions: $\dfrac{\partial T}{\partial y} = 0$ (6*e*)

It may be noted that for the overall heat transfer process from the air side to fluid in the tube, the thermal resistance of the inner fluid side is much less than that of the air side. In addition, the tube wall is made of copper, which has very high thermal conductivity. Thus, the assumption of constant tube wall temperature is a well-accepted practice in the literature even though the air-side local heat transfer coefficient around the tube periphery may be different.

Numerical Methods

The elliptic equations are solved by the full-field computational method. Because of the conjugated nature of the problem, the fin surfaces are considered as a part of the solution domain and will be treated as a special fluid with infinite

viscosity. To guarantee the continuity of the flux rate at the interface, the thermal conductivity of the fin and fluid adopt individual values, while the heat capacity of the fin surface takes the value of the fluid [14, 15]. The circular tube is approximated by the stepwise method; in order to guarantee its constant temperature, a very large value of the thermal conductivity is assigned to the tube region. Because of the complex geometry of slit fins, a special array called LAG is introduced to identify different regions, including fluid, fin base, tube, and strips. The computational domain is discretized by nonuniform grids, with the grids in the fin coil region being finer and those in the extended regions being coarser. Governing equations are discretized by the finite-volume method [14, 16]. In order to improve the efficiency and accuracy of the code, the convection term is discretized by the SGSD scheme [17]. The coupling between pressure and velocity is implemented by the CLEAR algorithm [18, 19]. The total grid points are $211 \times 85 \times 24$, and the grid independence study has been conducted by Cheng et al. [4]. The convergence criterion for the velocity is that the maximum mass residual of the cell divided by the inlet mass flux is less than 5.0×10^{-6}, and the criterion for temperature is that the difference between two heat transfer rates obtained from an iteration and after 50 successive iterations is less than 1.0×10^{-6}.

According to heat transfer theory [20, 21], the fin efficiency is defined as

$$\eta_{\text{fin}} = \frac{Q_{\text{real}}}{Q_{\text{ideal}}} \tag{7}$$

where Q_{real} is the actual heat transfer rate between the air and the fin surface and Q_{ideal} is the ideal heat transfer rate when the fin temperature is equal to the tube temperature T_{W}. To implement the ideal situation, we just artificially give the fin surface a very large value of thermal conductivity, say, 1.0×10^{30}, which leads to the results of uniform temperature of the fin surface equal to the value of the tube wall.

RESULTS AND DISCUSSION

Parameter Definitions

Some parameters are defined as follows:

$$\text{Re} = \frac{\rho u_m D_e}{\mu} \tag{8}$$

$$h = \frac{Q_{\text{real}}}{A\,\Delta T\,\eta_0} \tag{9a}$$

$$\eta_0 = (A_{\text{tube}} + A_{\text{fin}}\eta_{\text{fin}})/A \simeq \eta_{\text{fin}} (A_{\text{tube}}/A \simeq 0;\ A_{\text{fin}}/A \simeq 1) \tag{9b}$$

$$h_{\text{eff}} = h\eta_{\text{fin}} \tag{9c}$$

$$\text{Nu} = \frac{h_{\text{eff}} D_e}{\lambda} \tag{10}$$

$$Q_{\text{real}} = \dot{m} c_P (T_{in} - T_{\text{out}}) \tag{11}$$

$$\Delta p = p_{\text{in}} - p_{\text{out}} \tag{12}$$

$$f = \frac{\Delta p}{1/2 \rho u_m^2} \bullet \frac{D_e}{L} \tag{13}$$

$$\Delta T = \frac{T_{\max} - T_{\min}}{\log(T_{\max}/T_{\min})} \tag{14}$$

$$R = \frac{\Delta T}{Q} \tag{15}$$

where u_m is the mean velocity of the minimum transverse area, D_e is the outer tube diameter, T_{in} and T_{out} are the bulk temperature of the inlet and outlet of the fin surface, respectively, and $T_{\max} = \max(T_{\text{in}} - T_w, T_{\text{out}} - T_w)$, $T_{\min} = \min(T_{\text{in}} - T_w, T_{\text{out}} - T_w)$, and R is the thermal resistance.

It should be noted that the Nusselt number defined in Eq. (10) is the effective one, which is proportional to the actual heat transfer rate. For the comparison based on engineering applications, this effective Nusselt number is more convenient because it is related directly to the actual heat transfer rate. In the following presentation, this effective Nusselt number will be adopted.

Validation of the Code

The validation of the code has been done in our previous publication (see Figure 5 of Cheng et al. [4]); for the sake of simplicity it will not be presented here.

Comparison of Nusselt Numbers among Five Slit Fins

In Figure 4 we compare the Nusselt numbers of five slit fins under different Reynolds numbers ranging from 2.8×10^3 to 1.35×10^4, and corresponding frontal velocities ranging from 2 to 10 m/s. As expected, the increase of Nusselt numbers of the five slit fins becomes mild with increasing Reynolds numbers. It is interesting to note that slit 1, with all the strips located in the front part, has the poorest heat transfer performance, and following the order from slit 1 to slit 5, the Nusselt numbers increase at first, then, after reaching a maximum at slit 3, they begin to decrease. However, it should be noted that slit 5, with all the strips located in the rear part, still has a higher heat transfer rate than slit 1. The above numerically predicted results are in agreement with the experimental data provided by Kang and Kim [12] and the numerical results obtained by Qu et al. [3]. In the range of Reynolds numbers studied, the Nusselt numbers of slit 5 are about 7% higher than those of slit 1, and a similar phenomenon also appears for slit 2 and slit 4. Although they have symmetric strip arrangements on the fin surface, slit 4 also has 7% higher Nusslet numbers than slit 2. From the analysis presented above, we can see that strip

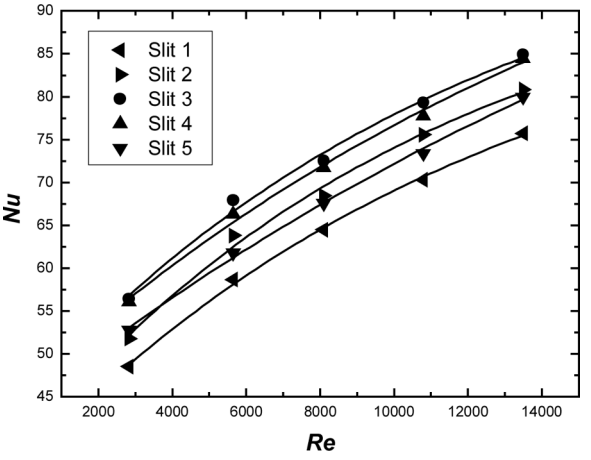

Figure 4. Comparison of Nu among five slit arrangements.

arrangement in the rear part is more effective than that in the front part. However, how can we find the optimum strip arrangement as slit 3, which can have 6% higher Nusselt number than slit 4? This is the major issue that is of concern in the present article and is discussed in the following presentation.

Comparison of Fin Efficiency

According to Eq. (7), we can get the fin efficiency of the five slit fins; the results are shown in Figure 5. The fin efficiency decreases with increase of the Reynolds number or frontal velocity. This is consistent with the common understanding of heat transfer theory [20, 21]. Similar to the heat transfer performance, following the order from slit 1 to slit 5, the fin efficiency increases at first, then, after reaching a maximum value at slit 3, it begins to decrease. Therefore, we know that for slit fins

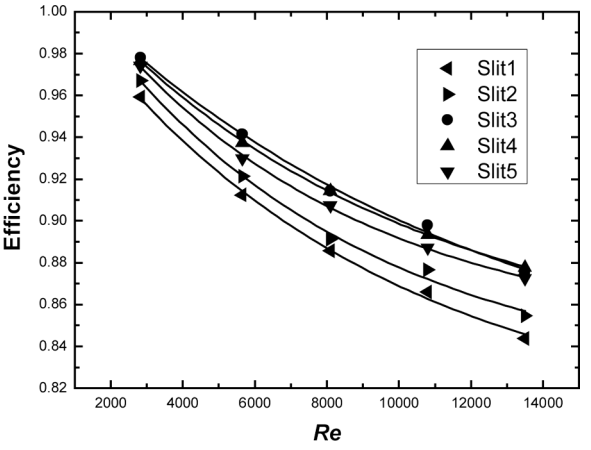

Figure 5. Comparison of fin efficiency among five slit arrangements.

with a fixed number of strips, the heat transfer performance can be attributed to some extent to the fin efficiency.

Comparison of Friction Factors

The variation of friction factors of the five slit fins with Reynolds number is shown in Figure 6, from which we can see that at low Reynolds number the differences in the friction factors are quite large, but when the Reynolds number increases, the differences are reduced. Because most strips of slit 1 and slit 2 lie in the inlet region, they can interrupt the fluid flow greatly, hence their friction effects are greater than those of slit 3, slit 4, and slit 5, for which most strips are located on the rear part, and this phenomenon is more obvious at high Reynolds numbers. However, under all the Reynolds numbers, slit 3 always has the lowest friction factor, and because its overall Nusselt number is also always the highest, slit 3 has the best overall performance.

Comparison of Front and Rear Thermal Resistances

For convenience, we divide the slit fins into two types equally along the flow direction. In order to investigate further the difference in heat transfer performance among the five slit fins, the thermal resistances in the front part and rear part are calculated according to Eq. (15); the results are shown in Figure 7. Following the order from slit 1 to slit 5, the number of strips on the front surface decreases, hence the corresponding thermal resistance increases. Similarly, following the same order from slit 1 to slit 5, because more strips are arranged on the rear part, the heat transfer performance increases there, so the thermal resistance in the rear part decreases. The overall heat transfer performance depends on the combination of the two thermal resistances, in the front part and the rear part. It is noticeable that the front and rear thermal resistances of slit 3 are almost identical, which can account

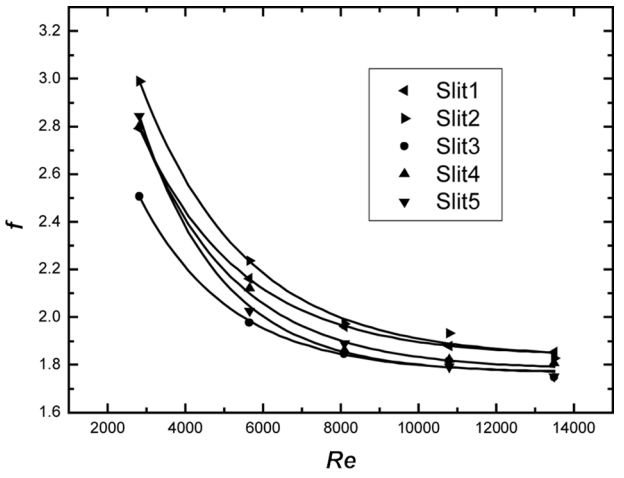

Figure 6. Comparison of friction factors among five slit arrangements.

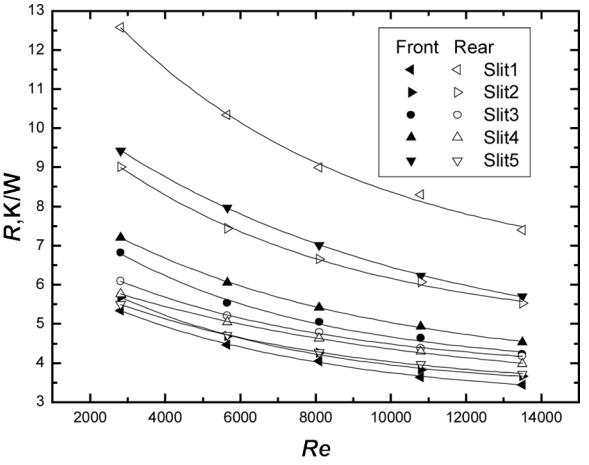

Figure 7. Comparison of front and rear thermal resistance among five slit arrangements.

for its highest Nusselt number among the five slit fins as follows. This discovery can be understood from heat transfer theory as follows.

For the heat transfer process from the air to the fin, along the flow direction two thermal resistances can be considered; one is between the air and the front part of the fin, and the other is between the air and the rear part of the fin. The two thermal resistances are connected in parallel, and they will determine the air-side thermal resistances. As we know from heat transfer theory [20], for an overall heat transfer process composed of several sections in series, the thermal resistances are serially connected, and among them one or two resistances may be the major ones. The most important thermal resistance should be first reduced in order to enhance the heat transfer. Once the most important thermal resistance is significantly reduced, the overall heat transfer will be greatly enhanced. For example, for the heat transfer from air to refrigerant, the thermal resistances include from air side to fin, from fin to tube, from tube outside to tube inside, and from tube inside to refrigerant. For the above-mentioned case, the air-side resistance and refrigerant-side resistance are larger than the conduction resistance in the fin and tube wall. And the air-side thermal resistance should first be reduced. The thermal resistance reduction of the first major one may cause the thermal resistance of the second major one to be in a relatively important position. When the two major thermal resistances are almost the same, the overall heat transfer performance will reach a nearly optimum situation. The so-called double enhanced tube for phase-change heat transfer is a typical application example of the above analysis [22]. This analysis can also be applied to each individual section when the thermal resistance of the section is composed of several parts connected in parallel. For slit 1, the main thermal resistance lies in the rear part, while for slit 5 the thermal resistance in the front part predominates (see Figure 7). Among the five strip arrangements, only slit 3 almost attains a balance of the thermal resistances in the front part and the rear part, hence it has the best heat transfer performance. This gives us a new guideline: Only when the thermal resistances in the front part and rear part

are nearly identical can the optimum fin be obtained. For the plain fin, because the main thermal resistance is located in the rear part, more strips should be arranged there to reduce the thermal resistance effectively. Hence the strip arrangement should abide by the rule of "front coarse and rear dense." With increase of strips in the rear part, the difference in thermal resistances between the front part and the rear part of the fin will be changed. The control of the degree of "coarse" and "dense" in the front and rear parts should be such that the two parts of thermal resistance are nearly the same. With this guideline, the design of an efficient fin need not be carried out only through trial and error; instead, we can obtain the nearly optimum fin when the thermal resistances between the front part and rear part are approaching each other.

Comparison of Ratios of Heat Transfer Rate Between Front Part and Overall Fin

Figure 8 shows the comparison of heat transfer ratio in the front part with the overall heat transfer rate. Because the temperature difference between the bulk air and the fin surface decreases along the flow direction, the heat transfer rate also decreases, so most of the heat transfer occurs in the front part. With increasing Reynolds number, the heat transfer ratio decreases. Following the order from slit 1 to slit 5, as fewer strips are arranged in the front part and more strips are put in the rear part, the heat transfer ratio also decreases, as shown in Figure 8. For slit 5, with the most strips in the rear part, the heat transfer rate is almost equal to that in the rear part at high Reynolds number.

Comparison of Ratios of Pressure Drop Between Front Part and Overall Fin

Figure 9 shows the pressure drop ratio in the front part to the total pressure drop. Unlike the heat transfer ratio above, the pressure drop ratio does not change

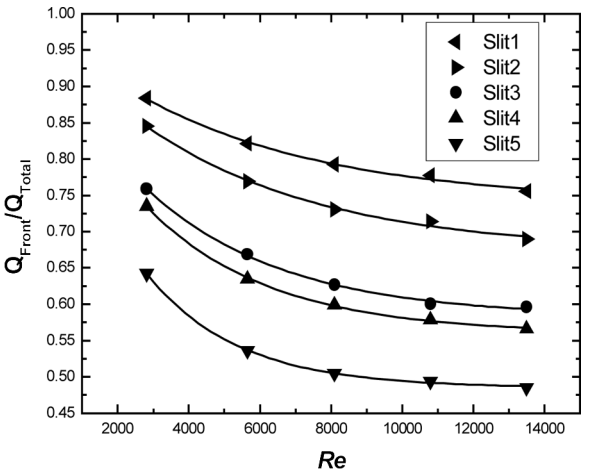

Figure 8. Comparison of ratios of front heat transfer rate and total heat transfer rate.

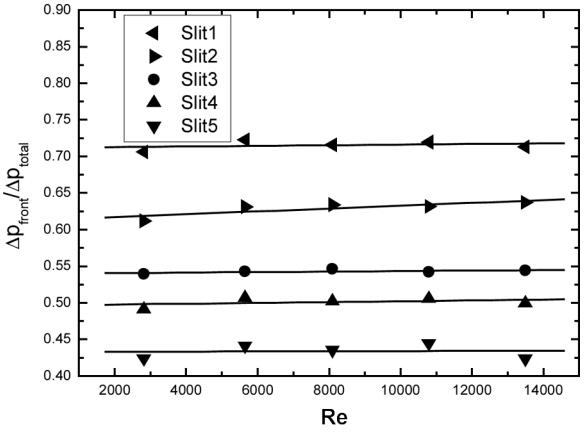

Figure 9. Comparison of ratios of front pressure drop and total pressure drop.

with increasing Reynolds number for all five slit fins. It is obvious that the more strips are in the front part, the higher will be pressure drop ratio. For slit 3, with the best overall performance, the pressure drop in the front part accounts for about 54% of the total pressure drop.

Influence of Fin Material on Fin Performance

The fin material has great influence on the heat transfer performance of the fins, especially for enhanced-heat-transfer fins. Here we investigate two types of fins of different materials; one is made of copper, whose thermal conductivity is 398 W/m K, and the other is made of an alloy with thermal conductivity of 18 W/m K, which is often used in some special fields, such as chemical processing. As we know, from the tube wall to the air there are two thermal resistances in series: One is the thermal resistance caused by the heat conduction in the fin, which depends on the fin geometry and thermal conductivity; the second is the convective resistance from the fin surface to the air, which is strongly dependent on the frontal velocity. Heat transfer enhancement is focused mostly on how to reduce the convective thermal resistance, and the conduction resistance is usually ignored. When the thermal conductivity of the fin is low, the conduction resistance can prevail in the overall heat transmission. Furthermore, after a slit fin is adopted, although the convective thermal resistance can be reduced greatly, the conduction resistance will definitely increase, so the slit fin may have only a small enhancement effect compared to the original plain fin, an effect that can be seen clearly in Figure 10. For a fin made of copper, the Nusselt numbers of the slit fin can be 60–100% higher than those of a plain fin; however, for a fin made of alloy, the Nusselt numbers of the slit fin can only be 10–20% higher than those of a plain fin.

From Figure 10 we can also see that the fin material has more influence on the slit fin than on the plain fin. For example, the Nusselt number of a plain fin made of alloy can be 50% less than that of a plain fin made of copper, while the Nusselt

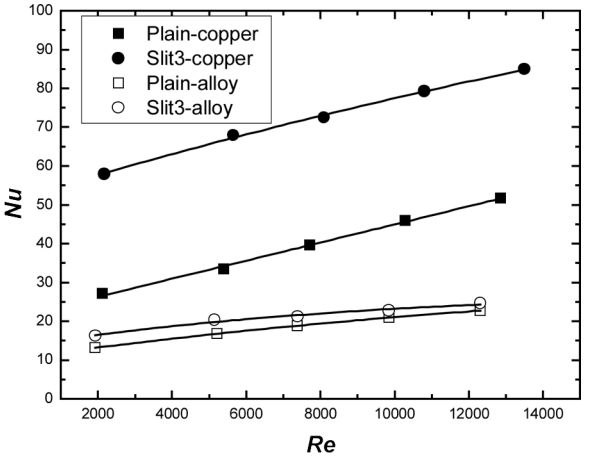

Figure 10. Nu of plain fins and slit fins with different fin materials.

number of a slit fin made of alloy is about 70% less than that of a slit fin made of copper. But, as expected, the fin materials does not influence the pressure drop, which is dependent only on the fin-tube geometry and fluid velocity. The predicted results of the friction factor for a plain fin and a slit fin are shown in Figure 11. In the whole Reynolds number range, the friction of the slit fin is about 40% higher than that of the plain fin.

The heat transfer performance of fins made of different materials can be attributed to the fin efficiency. From Figure 12, we can see that the fin efficiency of fins made of alloy is much lower than that of fins made of copper. It is very interesting to note that the slit fin made of copper has a higher fin efficiency than that of a plain fin made of copper at low Reynolds number, which can be explained as follows:

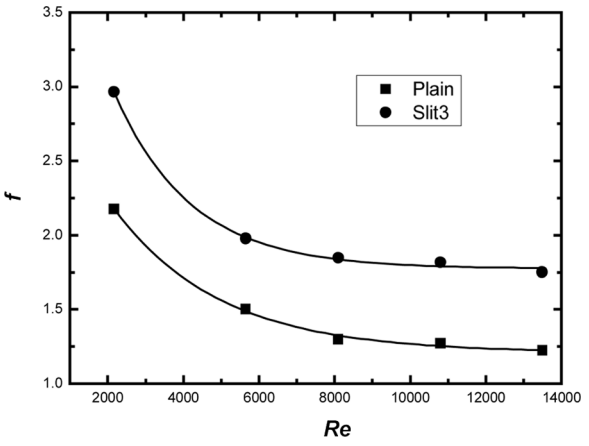

Figure 11. Computational results of *f* factor against Re.

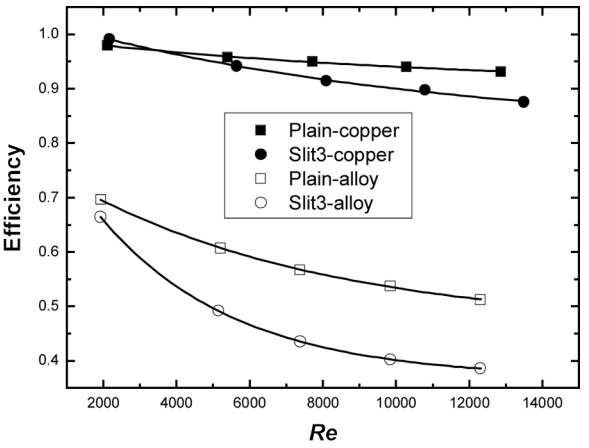

Figure 12. Fin efficiencies of plain fins and slit fins with different fin materials.

In the low-Reynolds-number region, the convective thermal resistance prevails and the slit fin has better convective heat transfer, leading to a higher heat transfer rate under the same temperature difference between the tube wall and the air, thus the fin efficiency of the slit fin is a bit higher than that of the plain fin. With an increase in frontal velocity, however, the convective thermal resistance decreases greatly while the conduction thermal resistance remains the same, hence the latter prevails. The existence of the strips on the slit-fin surface leads to an increase of the conduction thermal resistance of the fin, leading to a lower heat transfer rate, hence, the fin efficiency of the slit fin is lower than that of the plain fin when the Reynolds number is high. For the fins made of alloy, the conduction thermal resistance is always dominant, according to the above analysis, and the slit fin always has lower fin efficiency than the plain fin.

Finally, we would like to address one more issue. As can be seen from Eqs. (1)–(3), a steady-state model is adopted here. A question may arise as to whether the steady-state model is appropriate for the complicated geometry studied in this articles because vortex shedding may be formed and hence a transient model is required. This question has been answered in [23], where both a steady model and a transient model are used to simulate the plain fin-and-tube heat exchanger at $\mathrm{Re} = 5{,}000$. Those results showed that there is less than 1% difference in the average Nusselt number between the two models. Thus, in order to save computing resources, the steady model is adopted in this article.

CONCLUSIONS

In this article, the air-side heat transfer and pressure drop of five types of slit fins were investigated numerically with a three-dimensional laminar model, and the influence of the strip arrangement on the performance of slit fins was studied in detail. Then the numerical results were analyzed from the viewpoint of thermal resistance. The major conclusions are summarized as follows.

1. For the case of fixed strip number, when the strip density in the front part decreases and that in the rear part increases, the Nusselt number increases at first, then, after reaching a maximum, it begins to decrease, as does the fin efficiency.
2. The slit fin has the best heat transfer performance only when the thermal resistances in the front part and rear part are almost identical, which can be used as a second guideline to direct the design of enhanced-heat-transfer fins in conjunction with the principle of "front sparse and rear dense."
3. For five slit fins with different strip arrangements, the ratio of heat transfer rate in the front part to the overall heat transfer rate decreases with increasing Reynolds number, while the corresponding pressure drop ratio remains almost constant.
4. The fin thermal conductivity has a greater influence on the heat transfer performance of the slit fin than on that of the plain fin.

REFERENCES

1. W. Q. Tao, Z. Y. Guo, and B. X. Wang, Field Synergy Principle for Enhancing Convective Heat Transfer—Its Extension and Numerical Verifications, *Int. J. Heat Mass Transfer*, vol. 45, pp. 3849–3856, 2002.
2. W. Q. Tao, Y. L. He, Q. W. Wang, Z. G. Qu, and F. Q. Song, A Unified Analysis on Enhancing Convective Heat Transfer with Field Synergy Principle, *Int. J. Heat Mass Transfer*, vol. 45, pp. 4871–4879, 2002.
3. Z. G. Qu, W. Q. Tao, and Y. L. He, 3D Numerical Simulation on Laminar Heat Transfer and Fluid Flow Characteristics of Strip Fin Surface with X-Arrangement of Strips, *ASME J. Heat Transfer*, vol. 126, pp. 697–707, 2004.
4. Y. P. Cheng, Z. G. Qu, W. Q. Tao, and Y. L. He, Numerical Design of Efficient Slotted Fin Surface Based on the Field Synergy Principle, *Numer. Heat Transfer A*, vol. 45, pp. 517–538, 2004.
5. J. Y. Yun and K. S. Lee, Investigation of Heat Transfer Characteristics on Various Kinds of Fin-and-Tube Heat Exchangers with Interrupted Surfaces, *Int. J. Heat Mass Transfer*, vol. 42, pp. 2375–2385, 1999.
6. H. J. Kang, W. Li, H. J. Li, R. C. Xin, and W. Q. Tao, Experimental Study on Heat Transfer and Pressure Drop Characteristics of Four Types of Plate Fin-and-Tube Heat Exchanger Surfaces, *Int. J. Thermal Fluid Sci.*, vol. 3, no. 1, pp. 34–42, 1994.
7. W. Nakayama and L. P. Xu, Enhanced Fins for Air-Cooled Heat Exchangers—Heat Transfer and Friction Factor Corrections, *Proc. 1983 ASME-JSME Thermal Engineering Conf.*, vol. 1, pp. 495–502, 1983.
8. K. Hiroaki, I. Shinichi, A. Osamu, and K. Osao, High-Efficiency Heat Exchanger, *Natl. Tech. Rep.*, vol. 35, pp. 653–661, 1989.
9. C. C. Wang, W. H. Tao, and C. J. Chang, An Investigation of the Air Side Performance of the Slit Fin-and-Tube Heat Exchangers, *Int. J. Refrig.*, vol. 22, pp. 595–603, 1999.
10. Y. J. Du and C. C. Wang, An Experimental Study of the Airside Performance of the Superslit Fin-and-Tube Heat Exchangers, *Int. J. Heat Mass Transfer*, vol. 43, pp. 4475–4482, 2000.
11. J. Y. Yun and K. S. Lee, Influence of Design Parameters on the Heat Transfer and Flow Friction Characteristics of the Heat Exchanger with Slit Fins, *Int. J. Heat Mass Transfer*, vol. 43, pp. 2529–2539, 2000.
12. H. C. Kang and M. H. Kim, Effect of Strip Location on the Air-Side Pressure Drop and Heat Transfer in Strip Fin-and-Tube Heat Exchanger, *Int. J. Refrig.*, vol. 22, pp. 302–312, 1998.

13. T. W. H. Sheui, S. F. Tsai, and T. P. Chiang, Numerical Study of Heat Transfer in Two-Row Heat Exchangers Having Extended Fin Surfaces, *Numer. Heat Transfer A*, vol. 35, pp. 797–814, 1999.
14. W. Q. Tao, *Numerical Heat Transfer*, 2nd ed., Xi'an Jiaotong University Press, Xi'an, China, 2001.
15. W. Q. Tao, *Recent Advances in Computational Heat Transfer*, Science Press, Beijing, 2000.
16. S. V. Patankar, *Numerical Heat Transfer and Fluid Flow*, McGraw-Hill, New York, 1980.
17. Z. Y. Li and W. Q. Tao, A New Stability-Guaranteed Second-Order Difference Scheme, *Numer. Heat Transfer B*, vol. 42, pp. 349–365, 2002.
18. W. Q. Tao, Z. G. Qu, and Y. L. He, A Novel Segregated Algorithm for Incompressible Fluid Flow and Heat Transfer Problems—CLEAR (Coupled & Linked Equations Algorithm Revised) Part I: Mathematical Formulation and Solution Procedure, *Numer. Heat Transfer B*, vol. 45, pp. 1–17, 2004.
19. W. Q. Tao, Z. G. Qu, and Y. L. He, A Novel Segregated Algorithm for Incompressible Fluid Flow and Heat Transfer Problems—CLEAR (Coupled & Linked Equations Algorithm Revised): Part II: Application Examples, *Numer. Heat Transfer B*, vol. 45, pp. 19–48, 2004.
20. F. P. Incropera and D. A. DeWitt, *Introduction to Heat Transfer*, 3rd ed., Willy, New York, 1996.
21. S. M. Yang and W. Q. Tao, *Heat transfer*, 3rd ed., Higher Education Press, Beijing, 1998.
22. T. H. Ooi, D. R. Webb, and P. G. Heggs, A Dataset of Steam Condensation over a Double Enhanced Tube Bundle under Vacuum. *Appl. Thermal Eng.*, vol. 24, pp. 1381–1393, 2004
23. Y. L. He, W. Q. Tao, F. Q. Song, and W. Zhang, Three-Dimensional Numerical Study of Heat Transfer Characteristics of Plain Plate Fin-and-Tube Heat Exchangers from View Point of Field Synergy Principle, *Int. J. Heat Fluid Flow*, vol. 26, pp. 459–473, 2005